A Low-complexity Feed-forward I/Q Imbalance Compensation Algorithm

Niels A. Moseley and Cornelis H. Slump
University of Twente
Signals and Systems Group
Department of Electrical Engineering
Mathematics and Computer Sciences (EEMCS)
Enschede
The Netherlands

Abstract— **This paper presents a low-complexity adaptive feed-forward I/Q imbalance compensation algorithm. The feed-forward solution has guaranteed stability. Due to its blind nature the algorithm is easily incorporated into an existing receiver design. The algorithm uses three estimators to obtain the necessary parameters for the I/Q imbalance compensation structure. The algorithm complexity is low due to 1-bit quantization in the estimators. Simulations show that the compensation algorithm is able to attain an image-rejection ratio (IRR) of up to 65 [dB] under various imbalance conditions.**

I. Introduction

Direct-conversion receivers [1] employing I/Q processing have become popular in recent years. Figure I shows a block diagram of an image-rejection direct-conversion receiver architecture. In the ideal case, these receivers have an implementation advantage over superheterodyne [2] [1] architectures because they do not require image filtering [3] [1].

The receiver architecture depicted in Fig. I is able to completely reject the image band when two conditions are satisfied. First, the local oscillator (LO) must produce signals with a phase difference of exactly 90° degrees. Second, the gains and phase responses of the I and Q branches must be matched.

Unfortunately, the requirements mentioned above are impossible to meet in practice. Mismatches in analog components cause an imbalance in the gain and phase responses of the branches. Therefore, the image band can no longer be rejected completely.

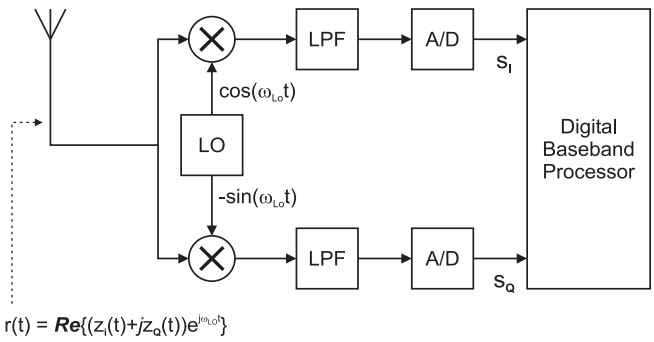

Fig. 1. A direct-conversion image-reject receiver architecture.

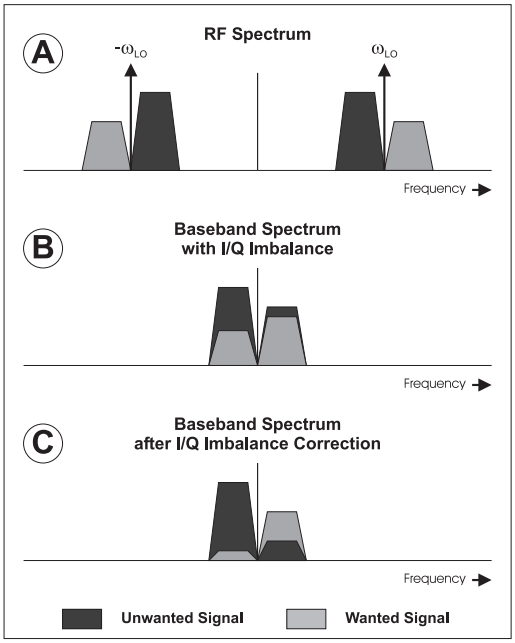

Fig. 2. RF and baseband spectra in several stages of a low-IF receiver.

Figure I shows the signal spectra at three stages within the receiver. In 'A' the RF spectrum at the antenna is shown. An unwanted signal is present in the channel adjacent to the wanted signal. The receiver is operating in a low-IF mode. Therefore the adjacent channel is the image band of the mixer.

In 'B' the baseband spectrum after down-mixing is shown. Due to the I/Q imbalance the image band, i.e. the unwanted signal, is insufficiently suppressed causing interference to the wanted signal.

After I/Q imbalance compensation the baseband spectrum looks like 'C'. The I/Q imbalance compensator increases the image-rejection ratio of the receiver. Now, the unwanted signal causes much less interference to the wanted signal.

In this paper we describe a blind feed-forward I/Q imbalance compensation algorithm. The benefit of a feed-forward solution is that it does not have the stability problems associated with feedback systems [4]. Furthermore, the blind nature of the algorithm makes the algorithm suit-

able to add onto an already existing receiver design.

The paper is organized as follows. Section II describes the I/Q imbalance model. In section III the structure of the compensator is explained. Section IV details the estimation of the model parameters after which section V discusses implementation aspects. Section VI presents some simulation results. Finally, section VII offers the conclusions.

II. I/Q imbalance model

We use the same I/Q imbalance model as described in [5]. The model assumes the I/Q imbalance is frequency independent. A parameter g amalgamates the gain mismatches between the branches of the receiver. And a parameter ϕ describes the phase mismatch of the LO, see Fig. 3.

In an I/Q imbalance scenario two baseband signals can be identified. The perfectly balanced complex baseband signal $z(t) = z_I(t) + jz_Q(t)$ and the complex baseband signal with I/Q imbalance $s(t) = s_I(t) + js_Q(t)$. The former is the baseband-equivalent signal at the antenna. The latter is the baseband signal seen by the digital baseband processor, see Fig I. Both baseband signals are related through the model parameters g and ϕ. The relation is shown by (1).

$$s(t) = K_1\, z(t) \;+\; K_2\, z^*(t) \tag{1}$$

where * denotes complex conjugation. And where

$$K_1 = \frac{1 + ge^{-j\phi}}{2} \tag{2}$$

$$K_2 = \frac{1 - ge^{j\phi}}{2} \tag{3}$$

are the complex baseband weighting coefficients.

In a perfectly balanced receiver $g = 1$ and $\phi = 0°$. This gives $K_1 = 1$ and $K_2 = 0$. Then, considering (1), $s(t) = z(t)$ which shows that the baseband-equivalent signal at the antenna equals the received baseband signal in the digital baseband processor.

Two important performance measures are the signal-to-interference ratio (SIR) and the image-rejection ratio (IRR). The IRR describes the amount of attenuation of

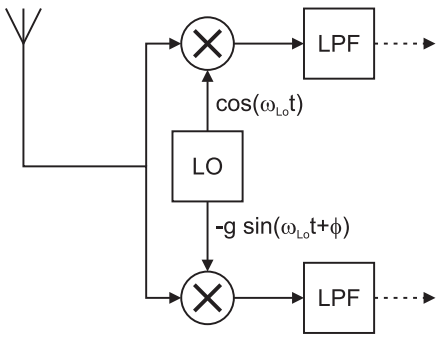

Fig. 3. The I/Q imbalance model with parameters g and ϕ.

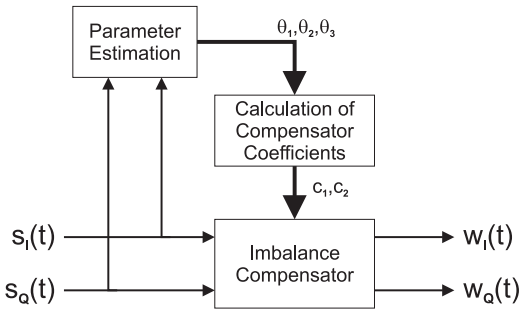

Fig. 4. The feed-forward compensation scheme.

the image frequency band as a function of g and ϕ. The IRR is expressed as

$$IRR = \frac{|K_1|^2}{|K_2|^2} = \frac{1 + 2g\,\cos(\phi) + g^2}{1 - 2g\,\cos(\phi) + g^2}. \tag{4}$$

The IRR of the image-rejection receiver in Fig. I is infinite under perfectly balanced conditions, i.e. $IRR = \infty$ when $g = 1$ and $\phi = 0$.

The SIR at baseband of our low-IF receiver model is expressed as

$$SIR = \frac{|K_1|^2}{|K_2|^2}\,\frac{P_s}{P_i} \tag{5}$$

where P_s is the power in the RF signal band and P_i is the power in the RF image band. The SIR describes the ratio between the power of the wanted signal and the power of the interference.

The minimum SIR needed to receive and decode a transmission correctly depends on the transmission standard.

III. I/Q imbalance compensation

Compensation of the I/Q imbalance is performed by the digital baseband processor. The compensation scheme is shown in Fig. 4. The complex baseband signal $s(t)$ is used to estimate three imbalance parameters θ_1, θ_2 and θ_3. In the proposed implementation this estimation process uses a simple block-based approach which is explained further in section V. The θ-parameters are used to calculate the coefficients required by the I/Q imbalance compensation structure.

To find the compensation structure, we start by splitting (1) into a real and imaginary part. This gives the expression [5] shown in (6) and (7).

$$s_I(t) = z_I(t) \tag{6}$$

$$s_Q(t) = g\,\cos(\phi) z_Q(t) - g\,\sin(\phi) z_I(t) \tag{7}$$

After some rearranging and letting $w(t) = z(t)$ to differentiate between the compensated signal and the original baseband signal $z(t)$ we get

$$w_I(t) = \lambda\, g\,\cos(\phi) s_I(t) \tag{8}$$

$$w_Q(t) = \lambda\, g\,\sin(\phi) s_Q(t) - \lambda\, g\,\cos(\phi) s_I(t) \tag{9}$$

where

$$\lambda = \frac{1}{g\,\cos(\phi)}$$

is an amplitude correction factor present in both branches and $w(t) = w_I(t) + jw_Q(t)$ is the compensated baseband signal.

The gain factor λ is not taken into account in the compensator shown in Fig. 5. In fact, it does not play a role in the I/Q imbalance phenomenon. It is assumed that this gain factor will be compensated by the channel equalizer at a later point in the receiver.

The compensator shown in Fig. 5 has two coefficients, namely

$$c_1 = g\,\sin(\phi) \tag{10}$$

and

$$c_2 = g\,\cos(\phi). \tag{11}$$

The compensation coefficients c_1 and c_2 are calculated from three estimates $\theta_{1\ldots3}$. The following section explains the calculation and estimation procedure.

IV. Calculation of the compensator coefficients

In the following sections it is assumed that z_I and z_Q are gaussian i.i.d random processes with variance σ^2 and zero mean.

The determination of the compensator coefficients c_1 and c_2 is achieved by first estimating the parameters $\theta_{1\ldots3}$. These parameters are defined as follows

$$\theta_1 = -E\{\mathrm{sgn}(s_I)\,s_Q\} \tag{12}$$
$$\theta_2 = E\{\mathrm{sgn}(s_I)\,s_I\} \tag{13}$$
$$\theta_3 = E\{\mathrm{sgn}(s_Q)\,s_Q\} \tag{14}$$

where $\mathrm{sgn}(x)$ is the sign function

$$\mathrm{sgn}(x) = \begin{cases} -1 & x < 0 \\ 0 & x = 0 \\ 1 & x > 0 \end{cases} \tag{15}$$

By using (6) and (7) and (10) and (11) the parameters can rewritten as

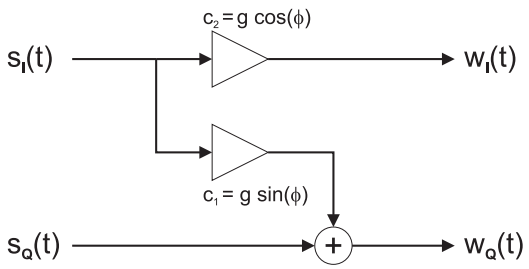

Fig. 5. The I/Q imbalance compensator structure.

$$\theta_1 = -E\{\mathrm{sgn}(z_I)\,s_Q\} \tag{16}$$
$$\theta_2 = E\{|z_I|\} \tag{17}$$
$$\theta_3 = E\{|s_Q|\} = E\{|c_2 z_Q - c_1 z_I|\} \tag{18}$$

Note that because the z_I and s_Q processes are gaussian distributed, $|z_I|$ and $|s_Q|$ are chi distributed [6] with one degree of freedom.

Now we will determine an analytical expression for each θ-parameter.

A. Examining θ_1

The expectation operator in (16) is expanded into a double integral.

$$\theta_1 = -\int_{-\infty}^{\infty}\int_{-\infty}^{\infty} s_Q\ \mathrm{sgn}(z_I)\ f_{s_Q,z_I}(s_Q, z_I)\ \ ds_Q\ dz_I \tag{19}$$

where $f_{s_Q,z_I}(s_Q, z_I)$ is the joint probability density function (pdf) of the random processes s_Q and z_I. The pdf is a bivariate gaussian distribution [7]. See the Appendix for a derivation of this joint pdf.

$$f_{s_Q,z_I}(s_Q, z_I) = \frac{1}{2\pi\sigma_1\sigma_2\sqrt{1-\rho^2}} \exp\left(-\frac{\frac{s_Q^2}{\sigma_1^2} - \frac{2\rho s_Q z_I}{\sigma_1\sigma_2} + \frac{z_I^2}{\sigma_2^2}}{2(1-\rho^2)}\right) \tag{20}$$

where

$$\rho = -\sin(\phi)$$
$$\sigma_1 = g\sigma$$
$$\sigma_2 = \sigma$$

According to [7] the expression in (19) can be written as (21) where the inner integral has been evaluated.

$$\theta_1 = -\frac{\rho\frac{\sigma_1}{\sigma_2}}{\sigma_2\sqrt{2\pi}} \int_{-\infty}^{\infty} \mathrm{sgn}(z_I) z_I \exp\left(\frac{-i^2}{2\sigma_2^2}\right)\ dz_I \tag{21}$$

The integral in (21) together with part of the normalization constant forms the equation for $E\{|z_I|\}$. The expectation of the absolute value of a zero mean gaussian distributed process X can be expressed as (22) [7].

$$E\{|X|\} = \sigma_x\sqrt{\frac{2}{\pi}} \tag{22}$$

By using (22) we arrive at (23).

$$\begin{aligned} \theta_1 &= -\rho\frac{\sigma_1}{\sigma_2}\sigma_2\sqrt{2\pi} \\ &= \sqrt{\frac{2}{\pi}}\,g\,\sigma\,\sin(\phi) \\ &= \sqrt{\frac{2}{\pi}}\,c_1\,\sigma \end{aligned} \tag{23}$$

B. Examining θ_2 and θ_3

An expression for θ_2 is easily found through direct application of (22).

$$\theta_2 = E\{|z_I|\} \tag{24}$$

$$= \sqrt{\frac{2}{\pi}}\sigma \tag{25}$$

The s_Q process is related to the processes z_I and z_Q through the coefficients c_1 and c_2. Thus, the s_Q process is zero mean gaussian distributed. The variance of the s_Q process depends on the variances of the z_I and z_Q processes as well as the covariance of z_I and z_Q.

$$\begin{aligned}\mathrm{var}(s_Q) &= \mathrm{var}(c_2\, z_Q - c_1\, z_I) \qquad (26)\\ &= c_2^2\,\mathrm{var}(z_Q) + c_1^2\,\mathrm{var}(z_I) + 2\,c_2\,c_1\,\mathrm{cov}(z_Q, z_I)\\ &= c_2^2\,\mathrm{var}(z_Q) + c_1^2\,\mathrm{var}(z_I)\\ &= g^2\,\sigma^2 \qquad (27)\end{aligned}$$

Using (27) with (28) gives (29).

$$\theta_3 = E\{|s_Q|\} \tag{28}$$

$$= \sqrt{\frac{2\,\mathrm{var}(s_Q)}{\pi}}$$

$$= g\,\sigma\,\sqrt{\frac{2}{\pi}} \tag{29}$$

C. Calculating the c-coefficients

The compensator coefficients c_1 and c_2 are obtained from the θ-parameters using (30) and (31).

$$c_1 = \frac{\theta_1}{\theta_2} \tag{30}$$

$$c_2 = \sqrt{\frac{\theta_3^2 - \theta_1^2}{\theta_2^2}} \tag{31}$$

It is also possible to obtain the parameters g and ϕ from the θ-parameters by means of (32) and (33) respectively.

$$g = \frac{\theta_3}{\theta_2} \tag{32}$$

$$\phi = \arcsin(\frac{\theta_1}{\theta_3}) \tag{33}$$

V. Implementation of the algorithm

In a practical realization the θ-parameters must be estimated. The following estimators are used to obtain estimates for the θ-parameters. Estimates are indicated by a hat over the symbol.

$$\hat{\theta}_1 = -\frac{1}{N}\sum_{n=1}^{N} sgn(s_I(n))\, s_Q(n) \tag{34}$$

$$\hat{\theta}_2 = \frac{1}{N}\sum_{n=1}^{N} sgn(s_I(n))\, s_I(n) \tag{35}$$

$$\hat{\theta}_3 = \frac{1}{N}\sum_{n=1}^{N} sgn(s_Q(n))\, s_Q(n) \tag{36}$$

where N is the number of samples used by each estimator.

Figure 6 shows a block diagram of an estimator. The sgn(.) operator extracts the sign-bit of the $in1$ input. The resulting signal is 1 bit wide. A multiplier changes the sign of the $in2$ signal depending on the output of the sgn(.) operator. The result is accumulated in a unit delay shown as z^{-1} by an adder.

In a VLSI realization the multiplier and adder are combined into a single adder/substractor where the sign bit of the $in1$ signal instructs the adder/subtractor to add or subtract the $in2$ signal. This implementation avoids the direct implementation of a high-speed multiplier.

After N accumulations, the content of the unit delay is passed to the output. The unit delay is reset and the cycle restarts. In effect, a new output is available from the estimator every N samples. This data-rate reduction means that the relatively complex calculations required to obtain the compensation coefficients c_1 and c_2 do not play a significant role in the algorithm's computational requirements.

Figure 7 shows a block diagram of the algorithm's implementation. It uses three estimators from Fig 6. Each estimator is followed by a lowpass filter to smooth its output. The smoothed outputs are used to calculate estimates for c_1 and c_2 using (30), (31).

Changing the cutoff frequency of the smoothing filter allows a trade-off between convergence speed of the algorithm and estimation accuracy.

VI. Simulation and Results

In this section, we evaluate the performance of the proposed algorithm and its implementation using MATLAB simulations by determining the signal-to-interference ratio before and after I/Q imbalance compensation. The SIR before I/Q imbalance compensation is calculated by (5). The SIR after I/Q imbalance compensation is determined through (37).

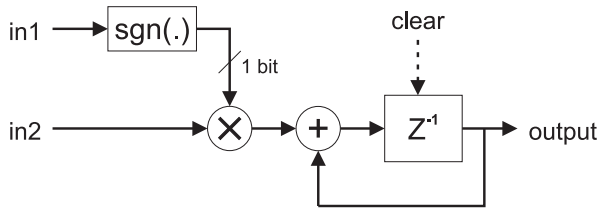

Fig. 6. The estimator using 1-bit quantization.

$$SIR_{post} = \left(\frac{|M_1^* K_1 - M_2 K_2^*|^2}{|M_1^* K_2 - M_2 K_1^*|^2} \right) \frac{P_s}{P_i} \tag{37}$$

where

$$M_1 = \frac{1}{2}\left(1 + \hat{g}\, e^{-j\hat{\phi}}\right) \tag{38}$$

$$M_2 = \frac{1}{2}\left(1 - \hat{g}\, e^{j\hat{\phi}}\right). \tag{39}$$

and K_1 and K_2 are defined by (2) and (3).

The parameters $\hat{g}$ and $\hat{\phi}$ are obtained from the simulation using (32) and (33).

The smoothing filters used after the estimators are identical one-pole lowpass types. Their z-domain transfer function is

$$H_{LP}(z) = \frac{0.01}{1 - 0.99\, z^{-1}}. \tag{40}$$

The frequency response of the smoothing filter is shown in Fig. 8.

Two I/Q imbalance scenarios were simulated using MATLAB. In the first scenario the receiver has 20% gain imbalance and 10° phase imbalance. In the second scenario it has 20% gain imbalance and 40° phase imbalance. The first scenario is indicative of a receiver with a traditional quadrature oscillator under serious imbalance conditions. The second scenario was chosen to show the applicability of the algorithm in receivers where the quadrature LO signal is made with a badly calibrated delay-line used as a phase shifter. See Fig. 9.

In Fig. 10(a) the SIR after I/Q imbalance compensation versus the SIR before I/Q imbalance is plotted for the first scenario. The θ-parameter estimators use blocks of $N = 256$ samples for each estimate. Figure 10(b) shows the results for the second scenario also with $N = 256$. Each SIR data point was obtained by averaging the results of 100 simulation runs.

Both plots in Fig. 10 show that the SIR after I/Q imbalance compensation is at least 50 [dB] higher than before compensation. At some points the SIR increase is as high as 65 [dB].

The convergence and tracking speed of the algorithm were evaluated with two simulation runs. The estimated

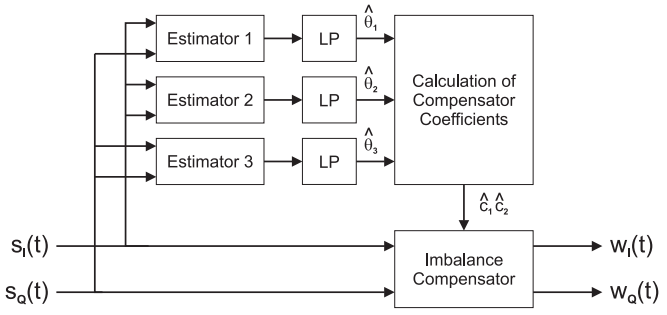

Fig. 7. Block diagram of the I/Q imbalance algorithm implementation.

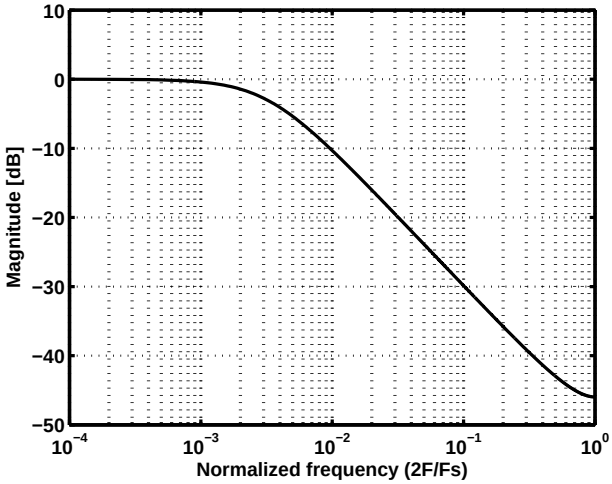

Fig. 8. Frequency response of the smoothing filter.

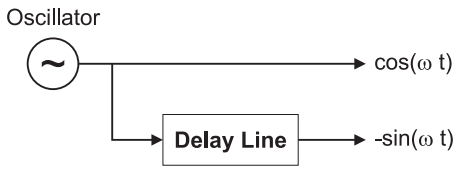

Fig. 9. Delay line based quadrature oscillator.

parameters $\hat{g}$ and $\hat{\phi}$ are plotted against time in Fig. 11. Also shown is the image-rejection ratio. The estimators were configured to use blocks of $N = 32$ and $N = 256$ samples for each estimate of the θ-parameters during the simulation run of Fig. 11(a) and Fig. 11(b) respectively.

The convergence times are an equal number of blocks in both simulation cases. In effect, the convergence speed of the algorithm is governed by the cutoff frequency of the estimator smoothing filters. The average IRR attained by the algorithm in the $N = 32$ case is comparable to the $N = 256$ case. This is due to the large amount of smoothing provided by the filters placed after the estimators. The filters reduce the variance of the estimators to such an extent that the effect of the block size parameter N is negligible.

The plots in Fig. 11 show that the algorithm generates parameters estimates $\hat{g}$ and $\hat{\phi}$ that follow the actual gain and phase imbalance parameters g and ϕ. Under both simulated I/Q imbalance conditions the algorithm is able to attain an IRR of at least 50 [dB] which is enough for certain applications, e.g. T-DAB [8].

VII. Conclusions

We have presented a blind adaptive feed-forward I/Q imbalance compensation algorithm that uses 1-bit quantization to avoid high-speed multipliers. The operating principle was explained by mathematical analysis of the three θ-parameters and the coefficients c_1 and c_2.

The convergence speed and accuracy of the algorithm are configurable by setting the cutoff frequency of the post-estimator smoothing filters. Although the estimator block length N has negligible effect on the accuracy of the al-

gorithm it is a useful parameter because it directly sets the rate at which the baseband processor must update the smoothing filters and the compensator coefficients. Therefore, it allows a trade-off between convergence speed and computational load.

The algorithm's performance was evaluated using MATLAB simulations. The simulations show that the algorithm is capable of attaining an image-rejection ratio of up to 65 [dB] under different I/Q imbalance conditions. Even when the phase imbalance is 40° the IIR after imbalance compensation is still above 50 [dB].

Appendix

[Joint probability density function derivation] We derive the joint probability density function $f_{s_Q,s_I}(s_Q, s_I)$ using Bayes' rule.

$$f_{s_Q,s_I}(s_Q, s_I) = f_{s_Q,z_I}(x, y) = f_{s_Q|z_I}(s_Q, z_I) \cdot f_{z_I}(z_I) \quad (41)$$

The probability density function of z_I, $f_{z_I}(z_I)$, is simply the gaussian distribution function

$$f_{z_I}(z_I) = \frac{1}{\sigma\sqrt{2\pi}} \exp\left(\frac{-z_I^2}{2\sigma^2}\right). \quad (42)$$

The conditional pdf $f_{s_Q|z_I}(s_Q, z_I)$ is derived using the fact that the I-channel value is given and may be interpreted as the conditional mean of the s_Q process, $\mathrm{E}\{\mathrm{s_Q}|\mathrm{z_I}\}$. As the s_Q process is gaussian distributed, determining the conditional variance, $\mathrm{var}\{\mathrm{s_Q}|\mathrm{z_I}\}$, is sufficient to describe the process.

Using (6) and (7), the conditional mean and variance are

$$\mathrm{E}\{\mathrm{s_Q}|\mathrm{z_I} = \mathrm{y}\} = -g \sin(\phi)\, y \quad (43)$$

$$\mathrm{var}\{\mathrm{s_Q}|\mathrm{z_I}\} = g^2 \cos^2(\phi)\, \sigma^2 \quad (44)$$

respectively.

The conditional pdf $f_{s_Q|z_I}(s_Q, z_I)$ is

$$f_{s_Q|z_I}(s_Q, z_I) = \frac{1}{\alpha\sigma\sqrt{2\pi}} \exp\left(\frac{-(s_Q + \beta z_I)^2}{2\alpha^2\sigma^2}\right) \quad (45)$$

where

$$\alpha = g\, \cos(\phi)$$
$$\beta = g\, \sin(\phi)$$

By multiplying (45) by (42), we arrive at an expression for the joint pdf

$$f_{s_Q,z_I}(s_Q, z_I) = \frac{1}{2\pi\alpha\sigma^2} \exp\left(-\frac{s_Q^2 + 2\beta s_Q z_I + g^2 z_I^2}{2\alpha^2\sigma^2}\right) \quad (46)$$

Now, (46) can be rewritten as (20).

Acknowledgment

This work was made possible by the WiCOMM project which is part of the Dutch Freeband Communication program.

References

[1] T.H. Meng W. Namgoong. Direct-conversion RF receiver design. *IEEE Transaction on Communications*, 49(3):518–529, March 2001.

[2] A. Abidi. Direct-conversion radio transceivers for digital communications. *IEEE J. Solid-State Circuits*, 30:1399–1410, December 1995.

[3] B. Razavi. *RF microelectronics*. Prentice Hall, 1998.

[4] B. Friedland. *Advanced Control System Design*. Prentice Hall, 1996.

[5] V. Koivunen M. Valkama, M. Renfors. Advanced methods for I/Q imbalance compensation in communication receivers. *IEEE Transactions on Signal Processing*, 49(10):2335–2344, October 2001.

[6] B. Peacock M. Evans, N. Hastings. *Statistical Distributions*. Wiley-Interscience, 3rd. edition, 2000.

[7] A. Papoulis. *Probability, Random variables, and Stochastic Processes*. McGraw-Hill, 3rd edition, 1991.

[8] CENELEC. Characteristics of DAB receivers. EN 50248, 1999.

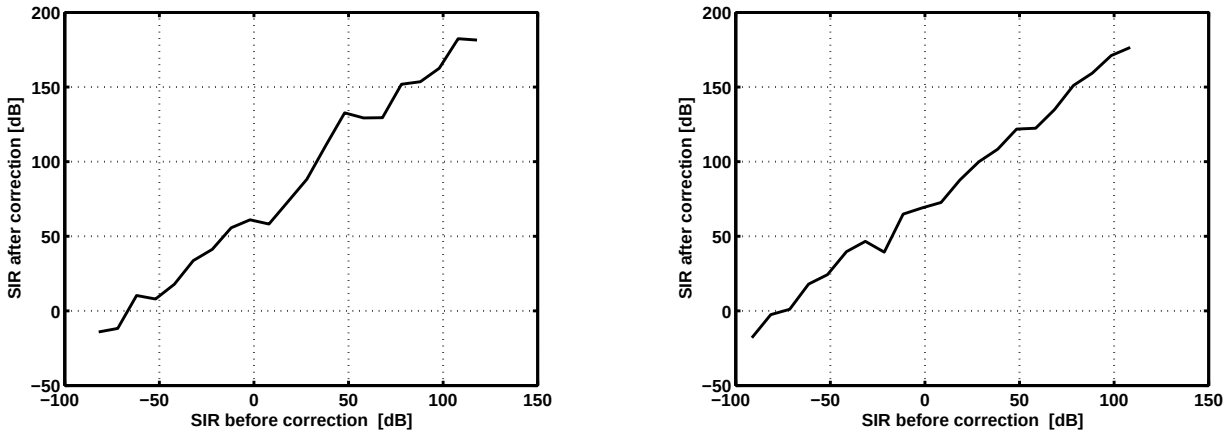

(a)$\phi = 10°$ (b)$\phi = 40°$

Fig. 10. Signal-to-interference ratio after versus before I/Q imbalance compensation. The parameters are $g = 1.2$ and $N = 256$.

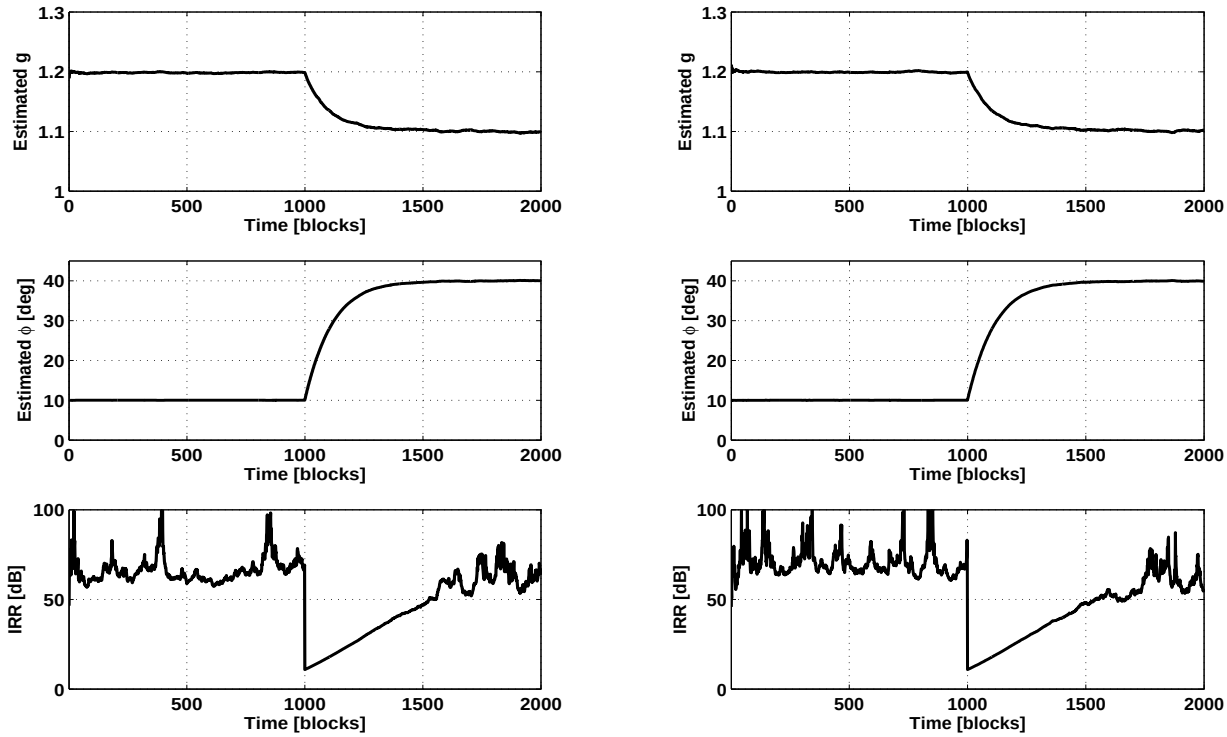

(a)$N = 32$ (b)$N = 256$

Fig. 11. Tracking simulation results. The run starts with $g = 1.2$ $\phi = 10°$. At time t=1000 blocks the I/Q imbalance parameters are changed to $g = 1.1$ $\phi = 40°$.